Published in final edited form as:
J Struct Biol. 2008 June ; 162(3): 404–410. doi:10.1016/j.jsb.2008.02.010.

Mechanical properties of mineralized collagen fibrils as influenced by demineralization

M. Balooch[1], **S. Habelitz**[1], **J. H. Kinney**[2], **S. J. Marshall**[1], and **G. W. Marshall**[1,*]

1 *Division of Biomaterials and Bioengineering, Dept. of Preventive and Restorative Dental Sciences, University of California, San Francisco, San Francisco, CA 94143-0758*

2 *Dept. of Mechanical Engineering, Lawrence Livermore National Laboratory, Livermore, CA*

Abstract

Dentin and bone derive their mechanical properties from a complex arrangement of collagen type I fibrils reinforced with nanocrystaline apatite mineral in extra- and intrafibrillar compartments. While mechanical properties have been determined for the bulk of the mineralized tissue, information on the mechanics of the individual fibril is limited. Here, atomic force microscopy was used on individual collagen fibrils to study structural and mechanical changes during acid etching. The characteristic 67 nm periodicity of gap-zones was not observed on the mineralized fibril, but became apparent and increasingly pronounced with continuous demineralization. AFM-nanoindentation showed a decrease in modulus from 1.5 GPa to 50 MPa during acid etching of individual collagen fibrils and revealed that the modulus profile followed the axial periodicity. The nanomechanical data, Raman spectroscopy and SAXS support the hypothesis that intrafibrillar mineral etches at a substantially slower rate than the extrafibrillar mineral. These findings are relevant for understanding the biomechanics and design principles of calcified tissues derived from collagen matrices.

Introduction

Mammalian mineralized tissues derived from the mesenchyme are based on a type-I collagen matrix that is reinforced by the incorporation of apatite mineral. The mineral forms in two distinguished spaces: a) intrafibrillar (within the collagen fibrils, preferentially in the gap zone between collagen molecules) and b) extrafibrillar (on the surface of the collagen fibril) (Landis et al, (1996). Both types of mineral are associated with the organic matrix of the tissue bound either directly to collagen or through a link facilitated by non-collagenous, most likely acidic, proteins. In bone it is thought that as much as 75% of the mineral is extrafibrillar (Bonar et al, 1985; Pidaparti et al., 1996). The partitioning of this mineral, that is, the relative amounts of mineral associated with each compartment is uncertain, and probably varies with the total levels of mineral in the calcified tissues. In Dentinogenesis Imperfecta type II (DI-II) dentin, which lacks intrafibrillar mineral, there is approximately 67% of the normal mineral level. (Kinney et al, 2001b:2003). Prior work on demineralization of dentin showed the development of a shoulder in the mineral profile, which is consistent with retention of about 35% of the mineral in the intrafibrillar compartment (Kinney et al, 1995), although this was not the original

*Corresponding author E-mail: gw.marshall@ucsf.edu.

interpretation of the finding. Thus there is significant evidence that most of the mineral is found in the extrafibrillar compartment.

Collagen fibrils display a characteristic 67 nm banded structure of gap and overlap zones (McEwen et al., 1992; Weiner and Wagner, 1998; Landis, 2002). The apatite crystals are believed to nucleate initially in the gap zone, followed by secondary mineralization of the interstitial positions between the fibrils (Landis et al, 1995) Mechanical properties of collagen fibrils in the fibril's long axis have been reported on mineralizing turkey leg tendon with varying degrees of mineralization, and increased dramatically with increased mineral content (Landis et al, 1995). The mechanical properties of the tissue depend on the degree of mineralization, although the relative importance of intra- and extrafibrillar mineral has not been established. There is some evidence, however, that intrafibrillar mineralization, is a dominant contributor to the elasticity and hardness of the tissue, even though it is the minor fraction of the mineral. In dry dentin lacking intrafibrillar mineral, a linear relationship between indentation modulus and mineral content was reported, similar to that seen in normal dentin; however this linear relationship vanished for the dentin without intrafibrillar mineral when the tissue was hydrated (Kinney et al, 2003). To explain these results we proposed that the extrafibrillar mineral acts as a granular material that can withstand load in dry tissue, but without intrafibrillar mineral when hydrated the capacity to sustain load is quite low (Kinney et al, 2003).

Atomic force microscopy (AFM) allows imaging in near-physiological conditions with nanometer resolution (Chen and Hansma, 2000; Hansma, 2001, Scheruring et al 2001; Marshall et al, 2001; Habelitz et al, 2002a). When applied to partially demineralized dentin, AFM reveals collagen fibrils of varying topographical profile (Habelitz et al, 2002a) that we hypothesize reflect different concentrations of the intrafibrillar mineral. Thus, smooth fibrils would contain the most intrafibrillar mineral and have the highest modulus, while fibrils with the typical 67 nm periodicity would have little or no mineral and a correspondingly lower modulus.

To determine if extrafibrillar mineral was removed before the intrafibrillar mineral, bulk dentin was monitored by Raman microspectroscopy and small angle x-ray scattering (SAXS) during acid etching. Subsequently, the rate of intrafibrillar demineralization in correlation with the topographic profiles of collagen fibrils was studied by AFM. In addition, we measured the indentation elastic modulus, E, along the collagen fibril axis using AFM to associate the fibril topography with modulus changes.

Materials & Methods

Tooth specimens were obtained from the UCSF Dental Hard Tissue Specimen Core, sterilized with gamma irradiation (White et al, 1994) and stored intact in de-ionized water and thymol at 4 °C until use. All specimens were non-carious human third molars that were extracted as required for dental treatment in compliance with a protocol approved by the Institutional Review Board at the University of California, San Francisco.

Raman Microspectroscopy and Small Angle X-Ray Scattering Studies (SAXS)

Raman microspectroscopy (HR 800 Raman, Jobin Yvon, Horiba, Japan) was carried out on dentin powder at different intervals during demineralization for up to 35 minutes in 10% citric acid to determine how long a detectable phosphate peak persisted. Approximately forty human third molars extracted form patients between 18 and 40 years of age were used. Enamel cusps and dentin roots were cut off using a diamond saw leaving behind mainly mid-coronal dentin. Residual enamel was removed using a diamond bur and the pulp chamber was cleaned using a dental scaler. Samples were air-dried immersed into liquid N_2 for 15 sec and then crushed into millimeter sized pieces. The dentin chips were subsequently milled in a ceramic ball mill

for 24 hours at low temperature. The dentin powder was sieved and the fraction smaller than 1 μm was used for these experiments. About 12 g of dentin powder were obtained. Specimens for each demineralization experiment consisted of 50 mg of 1 μm sized powder particles; the powder was placed in a 5 ml centrifuge test tube with a 0.22 μm filter (Ultrafree-MC, Millipore, USA) and 10 % citric acid was added to the test tube and demineralization initiated. Deionized water was added at a specific demineralization time and immediately centrifuged at 2000 rpm for 1 minute. This process was repeated to ensure that all acid was eliminated from the dentin powder. Demineralization increments were 2 to 3 minutes. The 50 mg powder specimen for each demineralization time was prepared individually and the whole set of demineralization studies for periods up to 35 minutes was repeated twice. Raman spectra were obtained from powder that was removed from the centrifuge test tube and placed on microscope glass slides. The spectrometer was operated with monochromatic radiation emitted by a He-Ne laser (632.8 nm) at 20 mW. Spectra were obtained after focusing the laser beam using a 100x optical lens (Nikon). Spectra between 600 and 1600 cm^{-1} were collected for 120 seconds and averaged over five repeats.

The SAXS studies were conducted on 0.25 mm thick sections cut perpendicular to the occlusal surface of the third molar using a slow-speed water cooled diamond saw (Isomet, Buehler Ltd., Lake Bluff, IL). SAXS patterns were obtained from identical locations before and after demineralization conducted over 16 hours in 10% citric acid. As shown in Fig. 2, the two external surfaces were demineralized leaving an unetched central portion of the section. SAXS was performed on beamline 4–2 at Stanford Synchrotron Radiation Laboratory. The x-ray beam was focused to a 250 μm spot size. Details of the experimental procedure have been described previously (Kinney et al, 2001a).

Single Collagen Fibril Studies of Demineralization and Mechanical Properties

Occlusal sections of 1–2 mm were cut with a low speed water cooled diamond saw (Isomet, Buehler Ltd., Lake Bluff, IL). The specimens were etched in 10% citric acid for 20 s to remove extrafibrillar mineral to a depth of about 1 μm based on prior demineralization rate studies (Marshall et al, 2001). We used ultramicrotomed (Model EM, UC6, Leica Microsystems GmbH, Wetzlar, Germany Model: EM UC6. with 3 mm diamond knifes) sections that were cut from the specimen and were extracted from the water bath behind the blade. Each section was then transferred onto a glass slide and exposed to continuous flow of water in a liquid cell of the AFM (Nanoscope IIIa, Veeco Instruments, Santa Barbara, CA) for one day prior to imaging by AFM. This exposure to water may have had a limited effect on the surface protein or mineral coating of the fibrils, as studies of enamel and dentin storage have shown a slow demineralization can occur in water (Habelitz et al, 2002b). Single fibers were identified and subsequently studied at various stages of demineralization and examined for their topographic profile and nanomechanical properties. Although many sections were examined we were able to conduct studies on three fibrils that were identified in this way and remained flat and stable throughout the experiments. After identification of a fibril, water was replaced by acid in the continuous flow liquid cell. At selected time intervals, acid was replaced by water again to stop the demineralization. At each interval the fibril was studied by AFM for topographic information (diameter and height variation between gap and overlap zones). At all times the fibrils were kept wet, either exposed to fresh water or acid. The AFM images were obtained with high aspect ratio Si tips in contact mode, since it provided good image quality and appeared not to induce fibril movement.

We also studied recombinant human type-I collagen fibrils as a zero mineral control. Recombinant human Type I collagen monomer was purchased from FibroGen, Inc (San Francisco, CA). The monomers were derived from genes for human Type I collagen α1 and α2 chains that were inserted into the genome of the yeast *Pichia pastoris* to produce

procollagen. The harvested procollagen was processed with protease to convert it to mature collagen and kept as monomer in acidic media. The recombinant collagen fibrils were assembled by diluting the purchased monomer stock to 100 μg/ml and dialyzing for 48 hrs against buffer (15.75 g/L NaCl, 13.76 g/L Tes-Buffer, 16.08 g/L $Na_2HPO_4{\cdot}7H_2O$) at room temperature, then dialyzing against water overnight at 4°C to remove salt from the solution. A drop of the solution was deposited on a glass slide or cleaved mica for five minutes, then washed with DI water and imaged in water using the same procedures described above for the dentin fibrils.

Indentation Modulus Determination of Collagen Fibrils

Collagen fibrils exhibiting different height profiles of the gap-overlap zones of the 67 nm repeat pattern during the demineralization experiments were studied to determine if the varying appearance indicated different mechanical properties as was expected if they contained differing mineral quantities. The indentations were determined using an AFM with pN force generating capability (PicoForce Nanoscope IIIa, Veeco, Inc. Santa Barbara, CA). After imaging an individual fibril in the liquid cell filled with deionized water, force displacement curves were taken along the long axis of the fibril at multiple points to determine the mechanical properties profile of the gap-overlap regions. Indentation modulus, E, was determined from force displacement curves. Deflection of the AFM cantilever was related to displacement of the piezo through a sensitivity factor, S, determined from deflection of the AFM tip on a quartz standard. The indentation, *X*, into the sample is the difference between the z-piezo movement, X_{dis}^{Piezo}, and the cantilever deflection, i.e.

$$X = X_{dis}^{Piezo} - S\,X_{def}^{c} \tag{1}$$

The force is assumed to be proportional to the cantilever deflection through spring constant *k* which was estimated from Sader's hydrodynamic model (Sader, 1998) and E, was evaluated following Sneddon's formulation (Sneddon, 1965) that is based on the geometry of a cylindrical cone indenting an elastic half space,

$$\mathrm{E} = \frac{\pi}{2}\frac{1-\nu^2}{\tan\varphi}\frac{F}{X^2} \tag{2}$$

where *F* is the force, *v* is the Poisson's ratio (assumed to be 0.5) and ϕ is the tip opening angle (18°).

Results

Powder and Bulk Demineralization

Raman spectra were obtained from dentin powder at different times of demineralization in 10% citric acid. The intensity of the v_1-mode of the PO_4 groups in apatite mineral at 960 cm^{-1} decreased with exposure time to the acid, as shown in Fig. 1. The peak intensity was reduced by about 80% after 10 min of acid exposure. After 29 min the peak at 960 cm^{-1} was not distinguishable from the background. The intensity of the phenylanine peak at 1007 cm^{-1} increased slightly in the first two minutes of etching, but remained constant at later times, perhaps due to released constraint on this group as mineral was removed. Thus it took approximately 30 min to remove all detectable mineral from 50 mg of powered dentin.

Small angle x-ray scattering (SAXS) studies were conducted before and after 16 hours of demineralization in 10% citric acid. Fig. 2A shows the x-ray beam penetrated through the external demineralized zones and an internal unetched zone after the demineralization treatment. Fig. 2B shows the SAXS patterns from unetched (top) dentin and after 16 h of etching (bottom). Prior to etching, background scattering from the extrafibrillar mineral partially obscured the intrafibrillar diffraction peak. As the extrafibrillar mineral was removed, the intrafibrillar peak became more pronounced against this scattering background (red arrows). Fig. 2C shows intensity profiles before and after etching, which resulted in the development of a pronounced peak at the 22 nm allowed harmonic of the 67 nm zone separation. The presence of a resolved peak associated with 67 nm periodicity of the fibrils indicates that mineral is regularly arranged in the gap zones (Kinney et al, 2001a). All of the other mineral (non-periodic) contributes to the general scattering background. The SAXS data provides key evidence that the extrafibrillar mineral is removed at a faster rate than is the intrafibrillar mineral.

Collagen Fibril Demineralization

AFM reveals only the topography of collagen fibrils. We believe intrafibrillar mineral assists in maintaining a smooth surface by filling the gap zones, while mineral removal causes the structure to assume topographic features of the gap and overlap zones seen in unmineralized collagen fibrils.

An isolated collagen fibril from human dentin is shown in Fig. 3A before controlled demineralization. The fibril appears smooth with little apparent periodicity. However, exposure to 10% citric acid gradually revealed periodicity over time such that a clear distinction between overlap and gap zones became apparent. This is shown in Figs. 3B–D at times up to 1600 s. Fig 4A shows the topographic profiles along the fibril axis (white lines in Fig 3) for the fibril shown in Fig. 3. The periodicity is close to 67 nm. The gap-overlap profile changed with demineralization starting from a flat profile (black data points). For short exposures, the profile appeared sinusoidal. The gap-overlap profile continued to increase in height with demineralization time until it reached about 6 nm between the peaks (overlaps) and valleys (gaps). After 1600 s, the gap portion of the profile became almost flat and did not change appreciably. The gap-overlap height difference as a function of $t^{1/2}$ is plotted in Fig. 4B**,** and its linearity suggests a diffusion-controlled process. Estimates of the diffusion coefficient based on the slope are about 10^{-14} cm^2/s.

Elastic Modulus Variations for Collagen Fibrils

We used recombinant human collagen type I as a control because it contains no mineral. The reconstituted fibrils tended to kink and not lie as straight as the dentin collagen fibrils, but still exhibited the typical periodicity of about 67 nm and cross-sectional profile similar to the decalcified human dentin fibrils (having 5–7 nm gap-overlap height). Fig. 5A shows a relatively straight section of a reconstituted fibril with the topographic profile (solid line) showing gap-overlap periodicity near 67 nm and a gap-overlap height of 5 nm. Modulus measurements (dotted line) along the fibril axis demonstrated a periodic variation of modulus values of approximately 30–35 MPa at the gaps and 60 MPa near the center of overlaps.

The modulus variation along a collagen fibril after demineralization in 10% citric acid for 3600 s is shown in Fig. 5B. The topographic profile (solid line) was similar to variations seen in the recombinant fibrils with gap-overlap height of about 6 nm. Modulus values measured along the fibril (dotted line) also varied from about 10 MPa in gap zones to 40 MPa near the center of the overlap zone, and had the normal fibril periodicity.

Fig, 5C shows an isolated fibril from normal dentin with intermediate topography after 240 s demineralization. The 67 nm periodic repeat pattern is apparent, but has a 2–3 nm gap-overlap height variation (solid line), with a narrow width to the region associated with the gap zone providing a sinusoidal appearance. The E variations (dotted line) were between 200 MPa near the gap to approximately 800 MPa in the overlap zone, between those in the demineralized fibrils and fibrils with apparently complete mineralization.

Fig. 5D shows an isolated fibril with a smooth appearance, in which the 67 nm period is barely detectable, suggesting the fibril is essentially fully mineralized. Modulus measurements along the fibril axis (dotted line) showed the typical undulating character seen in the fibrils without mineral (Fig 5A–B), but the magnitude of the E variations oscillated between 1.2 GPa in the gap zone to 1.5 GPa in the overlap zone.

The table summarizes the ranges of moduli measured on extracted collagen fibrils from three normal human third molars, along with those determined for numerous indentations made on recombinant collagen fibrils.

Discussion

A previous study (Kinney et al, 1995) in which demineralization was monitored dynamically with synchrotron radiation computed tomography, showed that dentin etching appeared to occur in two stages, each governed by an unique rate. About 70–75% of the mineral was removed rapidly, while the remaining mineral etched at a significantly slower rate. No satisfactory mechanism for the two-step behavior was proposed. However, since intrafibrillar mineral appears to make up 25–30% of the mineral (Bonar et al, 1985; Pidaparti et al., 1996), the two-step process is consistent with a much slower rate for intrafibrillar demineralization.

In this work, demineralization of fine dentin powder required prolonged exposure for complete mineral removal. In addition, demineralization of single collagen fibrils required periods of 2000–3600 seconds before gap-overlap height became constant, indicative of total mineral removal. The height change in the gap-overlap zone with demineralization time suggested a diffusion controlled process. However the estimated diffusion coefficient was orders of magnitude lower than would be expected for transport in a liquid medium. This suggests that the mineral within the fibrils is protected from the extracellular fluids. It may also reflect the indirect measurement of mineral removal by measurement of the fibril topography in which the volume change due to mineral removal is partially compensated by replacement with water or relaxation of the collagen fibril.

The elastic modulus of mineralized tissues depends on the amount of mineral deposited in the collagen matrix. From a simple rule of mixtures, one expects an increase in E with increasing mineral density (Currey, 1969, 1990). Experimental evaluation of the effect of intrafibrillar mineral on mechanical properties in dentin or bone has had limited attention due to the difficulty of its extraction, and problems associated with mechanical testing on single fibrils. Instead, as an approximation, mineralized turkey leg tendon (MTLT) has been studied since its collagen fibrils are arranged in a parallel fashion, and the tendon can be studied with varying degrees of mineralization depending on the age of the animal. Young's modulus increased more than two orders of magnitude with increasing mineral deposited in the collagen structure using the MTLT model (Landis et al, 1995). At the individual fibril level, the mechanical properties will also depend on the precise arrangement of the crystals within the fibrils (Weiner and Wagner, 1998; Rho et al, 1998). Jager and Fratzl (2000) further modified previous models for the mechanical properties of mineralized collagen fibrils (Wagner and Weiner, 1992) by introducing a staggered arrangement of mineral instead of mineral within the gaps in parallel arrangement. (Veis and Sabsay, 1987; Hulmes et al, 1995). Mineral contained within both gaps

and overlaps is consistent with the results of our work. Gupta et al (2006) recently reported tensile deformation characteristics that are in further agreement with the staggered model.

The moduli reported in the literature were mainly measured in the long axis of the fibrils (Landis et al, 1995). In our study, the E measured perpendicular to the fibril by indentation differs appreciably from that determined by tension in the axial direction, due to the fact that the indentation occurs into the fibril bulk. This increased contact compliance caused by the organic phase makes quantitative comparison of modulus values with previous studies unjustified. Tai et al (2005) used nanoindentation to measure elastic modulus of bone demineralized for various periods and reported 1.9 GPa for totally demineralized samples. However that work did not probe individual fibers and was carried out dry. If demineralized collagen from dentin (and presumably bone as well), is dried, the collagen network collapses and E values are dramatically elevated. Balooch et al (1998) found that when desiccated, demineralized dentin had values of about 2 GPa, but when wet the value for the static elastic modulus was 134 KPa. We did consider that the wet measurement of the collagen network was not a measurement of the demineralized collagen fibrils themselves, but this value is in the range of values we see in this study and points to the importance of hydration. Ankler et al (2004, 2005) reported the mechanical properties of dehydrated carious dentin increased approximately 100-fold for the modulus of elasticity compared with hydrated dentin, with the demineralized regions giving values of about 15 MPa, in approximate agreement with our values. Ho et al (2004) used nanoindentation to compare wet and dry elastic modulus of cementum and the cementum-dentin junction, which is less mineralized than cementum. On hydration the elastic modulus of cementum was reduced from 18.7 to 6.6 GPa and the less mineralized CDJ region was reduced from 17.5 to 3 GPa showing the dramatic effect of hydration. Furthermore, highly accurate indentation data for soft and compliant materials are quite difficult since we currently lack good standards and there are numerous complicating factors (Carillo et al, 2005). Finally although we know there is an important effect of hydration at the bulk level, we really do not understand the effect at the nanolevel at this time. Thus it is quite possible that the absolute values are not highly accurate, although the relative trends are thought to be reliable.

However, the present studies are in accord with the increases in E that accompany changes in mineral content reported by Landis et al, (1995). Using this indentation method we found a periodic variation in E that was associated with the periodic topographic variations along the fibril axes. Smooth fibrils gave the highest modulus values, and as topography increased with demineralization, the E variations became larger between the gap and overlap zones. The measured variations were correlated to the topographic variations and occasional deviations reflect experimental difficulty in precise location of the AFM tip on fibrils that are not perfectly flat.

Our findings confirm that mineral is located in two different compartments in collagenous mineralized tissues and reveal that the intrafibrillar mineral has a profound influence on the fibril topography and its mechanical properties. This study provided further evidence that intrafibrillar mineral is a major contributor to the strength of mineralized tissues and any attempt to remineralize or synthesize such tissues must provide for crystallization in the gap zones.

Acknowledgments

We thank Diana Zeiger for assistance with recombinant collagen preparation. This work was supported by the US Public Health Service through NIH/NIDCR Grants P01 DE09859 and R01 DE16849.

References

Angker L, Nijhof N, Swain MV, Kilpatrick NM. Influence of hydration and mechanical characterization of carious primary dentine using an ultra-micro indentation system (UMIS). Eur J Oral Sci 2004;112:231–236. [PubMed: 15154920]

Angker L, Swain MV, Kilpatrick N. Characterizing the micro-mechanical behavior of the carious dentine of primary teeth using nano-indentation. J Biomech 2005;38:1535–1542. [PubMed: 15922765]

Balooch M, Wu-Magidi IC, Lindquist AS, Balazs, Marshall SJ, Marshall GW, Seikhaus WJ, Kinney JH. Viscolelastic Properties of Demineralized Human Dentin in Water with AFM-Based Indentation. J Biomed Mater Res 1998;40 :539–544. [PubMed: 9599029]

Bonar LC, Lee S, Mook HA. Neutron diffraction studies of collagen in fully mineralized bone. J Molec Biol 1985;181:265–270. [PubMed: 3981637]

Carrillo F, Gupta S, Balooch M, Marshall SJ, Marshall GW, Pruitt L, Puttlitz C. Nanoindentation of polydimethylsiloxane elastomers: Effect of crosslinking, work of adhesion and fluid environment on elastic modulus. J Mater Res 2005:2820–2830.

Chen CH, Hansma HG. Basement membrane macromolecules: insights from atomic force microscope. J Struct Biol 2000;131:44–55. [PubMed: 10945969]

Currey JD. The relationship between the stiffness and the mineral content of bone. J Biomech 1969;2:477–480. [PubMed: 16335147]

Currey JD. Physical characteristics affecting the tensile failure properties of compact bone. J Biomech 1990;23:837–844. [PubMed: 2384495]

Gupta HS, Seto J, Wagermaier W, Zaslansky P, Boesecke P, Fratzl P. Cooperative deformation of mineral and collagen in bone at the nanoscale. Proc Natl Acad Sci U S A 2006;103:17741–6. [PubMed: 17095608]

Habelitz S, Balooch M, Marshall SJ, Balooch G, Marshall GW. In situ atomic force microscopy of partially demineralized human dentin collagen fibrils. J Struct Biology 2002a;138:227–236.

Habelitz S, Marshall GW, Balooch M, Marshall SJ. Nanoindentation and storage of teeth. J Biomechanics 2002b;35:995–998.

Hansma HG. Surface biology of DNA by atomic force microscopy. Annu Rev Phys Chem 2001;52:71–92. [PubMed: 11326059]

Ho SP, Balooch M, Goodis HE, Marshall GW, Marshall SJ. Ultrastructure and nanomechanical properties of cementum dentin junction. J Biomed Mater Res 2004;68A:343–351.

Hulmes DJS, Wess TJ, Prockop DJ, Fratzl P. Radial packing, order and disorder in collagen fibrils. Biophys J 1995;68:1661–1670. [PubMed: 7612808]

Jager I, Fratzl P. Mineralized collagen fibrils: A mechanical model with a staggered arrangement of mineral particles. Biophys J 2000;79:1737–1746. [PubMed: 11023882]

Kinney JH, Balooch M, Haupt DL, Marshall SJ, Marshall GW. Mineral distribution and dimensional changes in human dentin during demineralization. J Dent Res 1995;74:1179–1184. [PubMed: 7790595]

Kinney JH, Habelitz S, Marshall SJ, Marshall GW. The importance of intrafibrillar mineralization of collagen on the mechanical properties of dentin. J Dent Res 2003;82:957–961. [PubMed: 14630894]

Kinney JH, Pople JA, Marshall GW, Marshall SJ. Collagen orientation and crystallite size in human dentin: A small angle x-ray scattering study. Calcified Tissue Int 2001a;69:31–37.

Kinney JH, Pople JA, Driessen CH, Breunig TM, Marshall GW, Marshall SJ. Intrafibrillar mineral may be absent in Dentinogenesis Imperfecta Type II (DI-II). J Dent Res 2001b;80:1555–1559. [PubMed: 11499512]

Landis WJ. The structure and function of normally mineralizing avian tendons. Comparative BioChem Phys A 2002;133:1135–1157.

Landis WJ, Hodgens KJ, Song MJ, Arena J, Kiyonaga S, Marko M, Owen C, McEwen BF. Mineralization of collagen may occur on fibril surfaces: evidence from conventional and high-voltage electron microscopy and three-dimensional imaging. J Struct Biol 1996;117:24–35. [PubMed: 8776885]

Landis WJ, Librizzi JJ, Dunn MG, Silver FH. A study of the relationship between mineral content and mechanical properties of turkey gastrocnemius tendon. J Bone Mineral Res 1995;10:859–867.

Marshall GW, Yucel N, Balooch M, Kinney JH, Habelitz S, Marshall SJ. Sodium hypochlorite alterations of dentin and dentin collagen. Surface Science 2001;491:444–455.

McEwen BF, Song MJ, Landis WJ. Quantitative determination of the mineral distribution in different collagen zones of calcifying tendon using high voltage electron microscopic tomography. J Computer-Assit Microsc 1992;3:201–210.

Pidaparti RM, Chandran A, Takano Y, Turner CH. Bone mineral lies mainly outside collagen fibrils: prediction of a composite model for osteonal bone. J Biomech 1996;29:909–916. [PubMed: 8809621]

Rho J-Y, Kuhn-Spearing L, Zioupos P. Mechanical properties and the hierarchical structure of bone. Med Eng Phys 1998;20:92–102. [PubMed: 9679227]

Sader JE. Frequency response of cantilever beams immersed in viscous fluids with applications to the atomic force microscope. J Appl Phys 1998;84:64–76.

Scheuring S, Fotiadis D, Moller C, Muller SA, Engel A, Muller DJ. Single proteins observed by atomic force microscopy. Single Molecules 2001;2:59–67.

Sneddon IN. The relation between load and penetration in the axisymmetric Boussinesq problem for a punch of arbitrary profile. Int J Eng Sci 1965;3:47–57.

Tai K, Qi HJ, Ortiz C. Effect of mineral content on the nanoindentation properties and nanoscale deformation mechanisms of bovine tibial cortical bone. J Mater Sci Mater Med 2005;16:947–59. [PubMed: 16167103]

Veis, A.; Sabsay, B. The collagen of mineralized matrices. In: Peck, WA., editor. Bone and Mineral Research/5. Elsevier Science Publ. B.V.; New York, Amsterdam, Tokyo: 1987. p. 15

Wagner HD, Weiner S. On the relationship between the microstructure of bone and its mechanical stiffness. J Biomech 1992;11:1311–20. [PubMed: 1400532]

Weiner S, Wagner HD. The material bone. Structure-mechanical function relations. Annu Rev Material Sci 1998;28:271–298.

White JM, Goodis HE, Marshall SJ, Marshall GW. Sterilization of teeth by gamma radiation. J Dent Res 1994;73:1560–1567. [PubMed: 7929992]

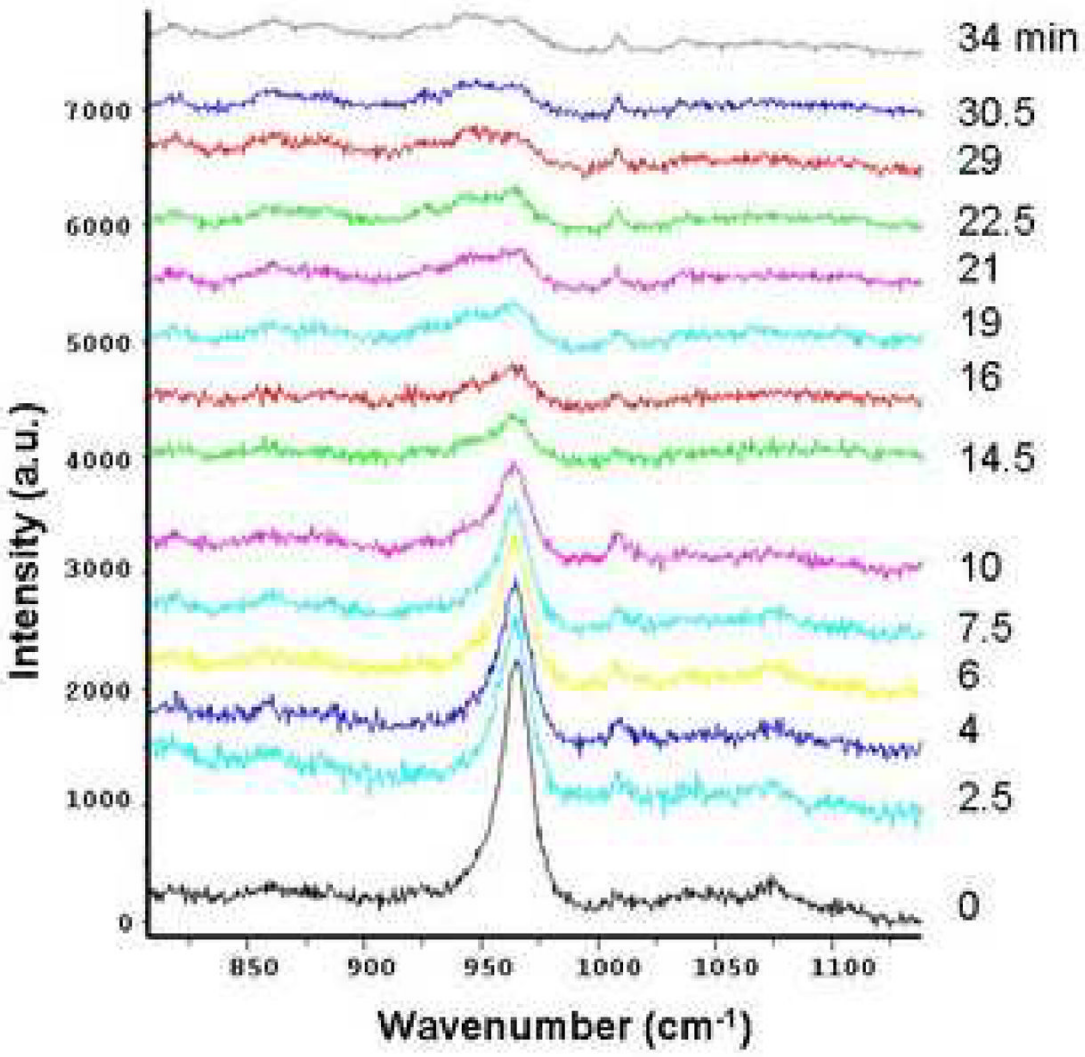

Figure 1.

Raman spectra during demineralization of 50 mg powder specimens of human dentin. The phosphate peak at 960 cm^{-1} decreased ~ 80% after 10 min. and was not distinguishable from background at 29 min. A small peak at 1007 cm^{-1} attributed to phyenylanine increased slightly in the first 10 min. and remained essentially constant subsequently.

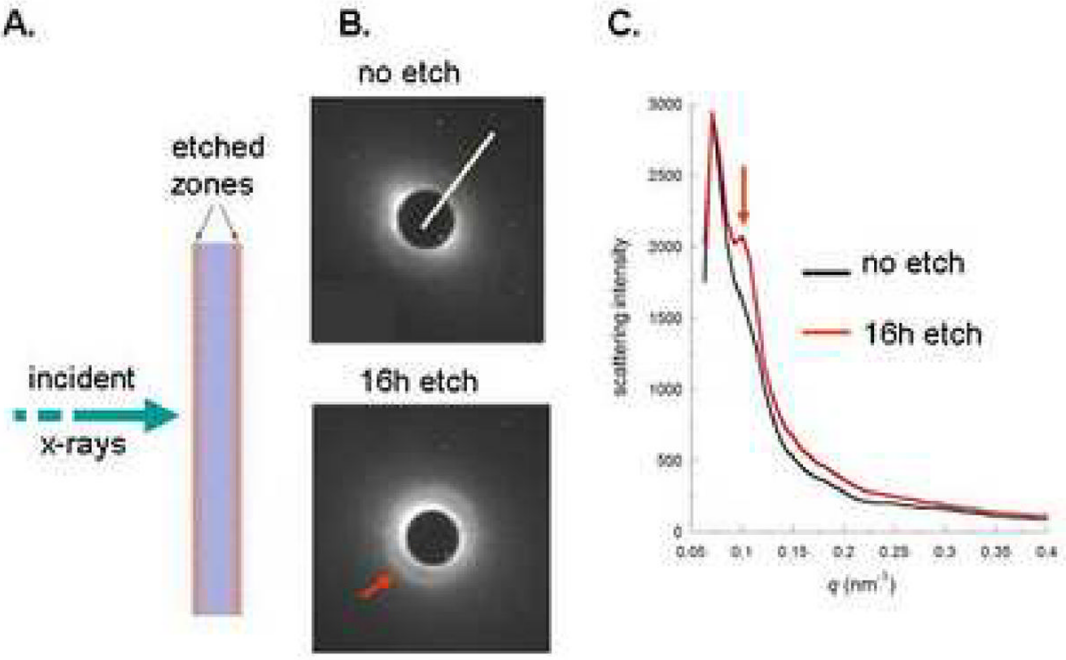

Figure 2.

SAXS experiment demonstrating enhancement of the 67 nm (22 nm third harmonic, red arrows) associated with intrafibrillar mineral in collagen fibrils. A. experimental set up showing x-ray beam penetrating the dentin slab. B. SAXS patterns were obtained after the beam penetrated the unetched dentin slab (top) and after etching (bottom) for 16 h in 10% citric acid so that the beam penetrated two surfaces that had been demineralized (etch zones in A.) and an unetched central core. White line in the top pattern shows the line used for the intensity profile. C. Intensity profiles before (black line) and after (red line) the 16 h etching experiment. Red arrows in B and C show the development of a pronounced peak associated with the third harmonic of scattering from the intrafibrillar mineral with 67 nm periodicity from apatite deposited in the gap zones of mineralized collagen fibrils (Kinney et al, 2001a). The SAXS profiles were adjusted so that the 16 h etch had the same maximum value as the unetched data. This normalization was helpful in order to show the difference between the two scattering curves in the same q range for scattering.

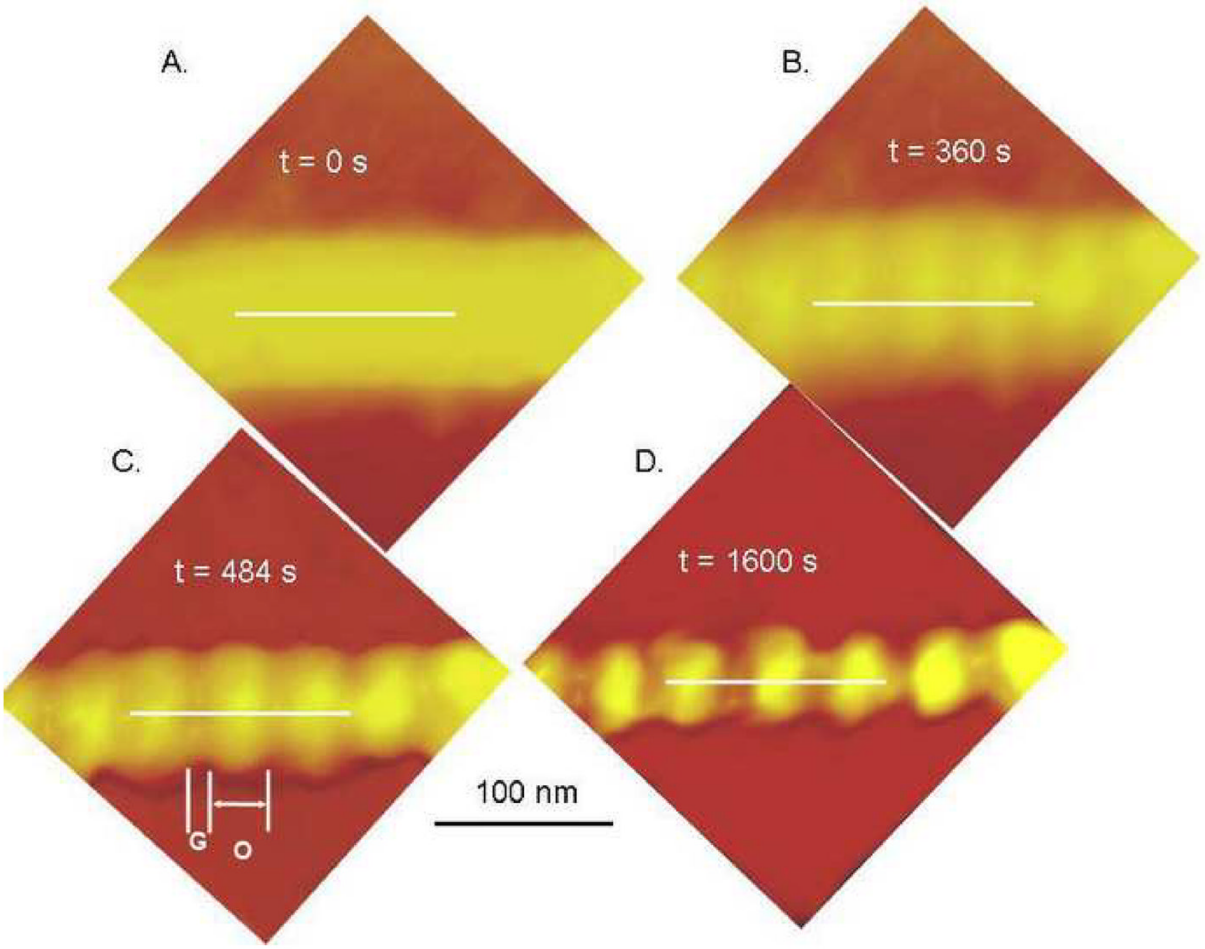

Figure 3.

Demineralization sequence in 10% citric acid of an isolated human dentin collagen fibril with white lines showing lines used to measure height variations in Fig. 4. A. initial appearance of the fibril was smooth and appeared to have indistinct boundaries. B. After 360 s of demineralization the underlying periodicity of the collagen fibril due to gap-overlap height differences was apparent. C. gap-overlap height differences increased with further demineralization at 484 s, labels G and O indicate gap and overlap zones, respectively. D.1600 s demineralization..

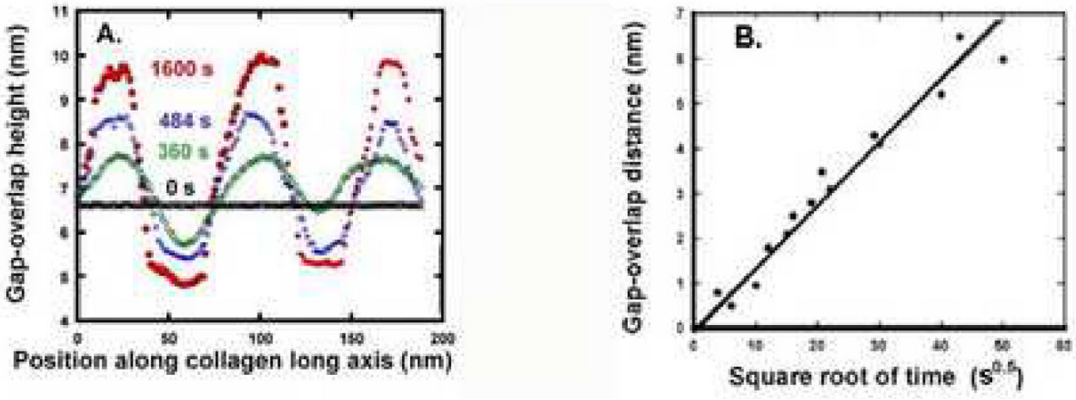

Figure 4.

A. Gap-overlap height differences of the collagen fibril shown in Fig. 3 (along white lines). The flat topography of the fibril (black line) increased with progressive demineralization shown at 360 s (green), 484 s (blue) and 1600 s (red). Similar results were seen in other fibrils demineralized for up to 3600 s. B. Gap-overlap distance increases with demineralization time for several human dentin collagen fibrils plotted vs. square root of time (s), suggesting a slow diffusion controlled process.

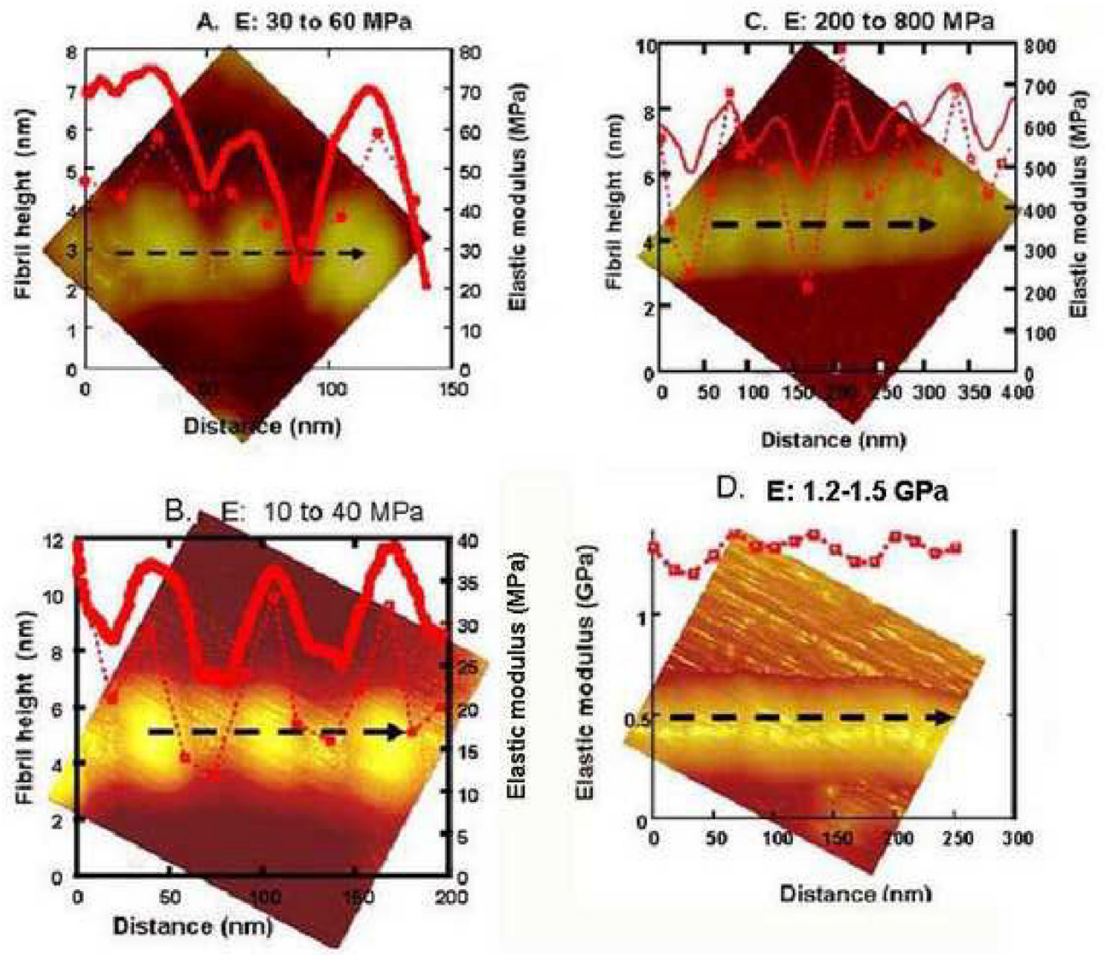

Figure 5.

AFM images associating topographic variations (solid red lines) with indentation elastic modulus values (broken red lines) along black dashed lines on isolated collagen fibrils with varying appearance. A. recombinant collagen fibril without mineral had gap-overlap height differences of 5 nm. Modulus values varied from about 30 MPa at gaps to 60 MPa at the overlaps. B. Fully demineralized human dentin collagen fibrils showing gap overlap height differences of about 6 nm and modulus variations between 10 MPa at gaps to 40 MPa in the overlap zones. C. Dentin collagen fibril after 240 s demineralization showing sinusoidal periodic variations in topography with gap-overlap height differences of 2–3 nm. Modulus values at the gaps were 200–400 MPa and at the overlaps were 500–800 MPa. D. Smooth dentin collagen fibril showing minimal gap-overlap height differences and modulus variations between 1.2 and 1.5 GPa.

Table

Collagen Fibril Source	Indentation Elastic Modulus Range
Dentin with varying intrafibrillar mineral N = 3	200 MPa- 2GPa
Dentin without intrafibrillar mineral N = 3	8–20 MPa
Reconstituted fibrils N = 3	30–50 MPa